Contrasting hydrological and thermal intensities determine seasonal lake-level variations – A case study at Paiku Co on the southern Tibetan Plateau

Yanbin Lei[1,2], Tandong Yao[1,2], Kun Yang[1,2,3], Lazhu[1], Yaoming Ma[1,2, 4], Broxton W. Bird[5]

[1] Key Laboratory of Tibetan Environment Changes and Land Surface Processes, Institute of Tibetan Plateau Research, Chinese Academy of Sciences, Beijing 100101, China
[2] CAS Center for Excellence in Tibetan Plateau Earth System, Beijing, 100101, China
[3] Department of Earth System Science, Tsinghua University, Beijing 10084, China
[4] University of Chinese Academy of Sciences, Beijing, China
[5] Department of Earth Sciences, Indiana University-Purdue University Indianapolis (IUPUI), Indianapolis, IN 46202, USA

Correspondence to: Yanbin Lei (leiyb@itpcas.ac.cn)

Abstract. Evaporation from hydrologically-closed lakes is one of the largest components of lake water budget, however, its effects on seasonal lake-level variations remain unclear on the Tibetan Plateau (TP) due to a lack of comprehensive observations. In this study, weekly lake evaporation and its effects on seasonal lake-level variations are investigated at Paiku Co on the southern TP using in-situ observations of thermal structure and hydrometeorology (2015-2018). Lake evaporation at Paiku Co was estimated to be 975±142 mm during the ice-free period (May to Dec), characterized by low values of 1.7±0.6 mm/day during the pre-monsoon season (May to Jun), high values of 5.5±0.6 mm/day during the post-monsoon season (Oct to Dec) and intermediate values of 4.0±0.6 mm/day during the monsoon season (Jul to Sep). There was ~5 months lag between the maximum lake evaporation (Nov) and maximum net radiation (Jun). These results indicate that the seasonal pattern of heat flux over the lake surface was significantly affected by the large lake heat storage. Contrasting hydrological and thermal intensities may play an important role in the large amplitude of seasonal lake-level variations at deep lakes like Paiku Co. High inflow from monsoon precipitation and glacier melting and moderate lake evaporation, for instance, drive rapid lake-level increase during the monsoon season. In contrast, high lake evaporation and reduced inflow cause lake level to significantly decrease during the post-monsoon season. This study further implies that lake evaporation may play an important role in the different amplitudes of seasonal lake-level variations between deep and shallow lakes and between the southern and northern TP.

1 Introduction

The Tibetan Plateau (TP) hosts the greatest concentration of high-altitude inland lakes in the world. More than 1200 lakes (>1 km^2) are distributed on the TP, with a total lake area of more than 45000 km^2 in the 2010s (Ma et al., 2011; Zhang et al., 2014a). During the past few decades, lakes on the TP experienced significant changes in response to climate warming, increased precipitation, glacier mass loss and permafrost thawing (Song et al., 2014; Lei and Yang, 2017). Most lakes on the interior TP have expanded dramatically since the late 1990s, in contrast with lake contraction on the southern TP (Lei et al., 2014). For most lakes across the TP, lake water temperature has also increased (Zhang et al., 2014b; Su et al., 2019), while lake ice duration has shortened considerably at the same time in response to rapid climate warming since the 1970s (Ke et al., 2013; Cai et al., 2017).

Compared to numerous studies of inter-annual to decadal lake changes, seasonal lake-level changes and the associated hydrological processes on the TP are less understood (Song et al., 2014). Phan et al. (2012) showed that seasonal lake-level variations on the southern TP were much larger than those on the northern and western TP. In-situ observations gave additional details of seasonal lake-level variations, showing that large lakes usually exhibited considerably greater seasonal lake-level variations relative to small lakes (Lei et al., 2017). For example, lake levels at Zhari Namco and Nam Co, two large and deep lakes on the central TP (Wang et al., 2009, 2010), increased significantly by 0.3~0.6 m during the summer monsoon season and decreased by a similar amount during the post-monsoon season. Two nearby relatively small and shallow lakes, Dawa Co and Bam Co, exhibited considerably less lake-level variability despite showing similar seasonal cycle (Lei et al., 2017). What caused these lake systems to experience different amplitudes of seasonal lake-level variations remains unstudied. Understanding how large and small lakes respond differently to similar forcing mechanisms is critical for understanding how continued warming will impact water storage on the TP. This work additionally may provide insight into discrepancies in lake-level reconstructions from large and small lakes on the TP that are used to reconstruct and understand long-term relationships between climate and water storage.

Evaporation from hydrologically-closed lakes is one of the largest components of lake water budget (Li et al., 2001; Morrill, 2004; Xu et al., 2009; Yu et al., 2011). Both the eddy covariance system and energy budget method are effective ways to determine lake evaporation (Blanken et al., 2000; Winter et al., 2003; Rouse et al., 2003, 2008; Lenters et al., 2005; Rosenberry et al., 2007; Giannoiu and Antonopoulos, 2007; Q. Zhang et al., 2014; Sugita, 2014, 2019). On the TP, several studies have used eddy covariance system to estimated lake evaporation, e.g. Nogring Lake (Li et al., 2015), Qinghai Lake (Li et al., 2016), Nam Co (Wang et al., 2017, 2019), Siling Co (Guo et al., 2016). Their results show that the seasonal pattern of lake evaporation is significantly affected by lake heat storage, especially for deep lakes. At Nam Co, for example, Haginoya et al. (2009) found that the sensible and latent heat fluxes were small during the spring and early summer, and increased considerably during the autumn and early winter due to the large heat storage. However, lake evaporation during the late autumn and early winter is not typically investigated using eddy covariance system because it is difficult to maintain the measurement platform due to the influence of lake ice. Likewise, energy budget studies that investigate changes in lake

65 heat storage and its effects on lake evaporation have been limited on the TP due to a lack of comprehensive in-situ observations. Although the energy budget method needs significant personnel commitment for fieldwork, it is more suitable for accurate, long-term monitoring of lake evaporation (Winter et al., 2003).

To fully understand the process that affects lake water budgets on the TP, we conducted comprehensive in-situ observations at Paiku Co, a deep alpine lake on the southern TP since 2013. In this study, lake evaporation at Paiku Co during the ice-free
70 period is estimated through energy budget (Bowen ratio) method and its effects on seasonal lake-level variations are investigated. We first address the thermal regime and changes in lake heat storage based on three years' water temperature profile data (2015-2018), then investigate energy budget and heat flux over the lake surface, and finally analyze the seasonal pattern of lake evaporation and its impact on seasonal lake-level variations. On the bases of these studies, the effects of lake evaporation on the different amplitude of seasonal lake-level changes between deep and shallow lakes and between the
75 southern and northern TP is discussed.

2 Methodology

2.1 Site description

Paiku Co (85 °35.12' E, 28 °53.52' N, 4590m a.s.l) is a hydrologically closed lake on the southern TP with a surface area of 280 km^2, watershed area of 2376 km^2, and salinity of 1.7 g/L. Bathymetry survey showed that the lake has mean water depth
80 of 41.1 m with the maximum water depth of 72.8 m (Lei et al., 2018). Glaciers are well developed to the south of the lake, with a total area of ~123 km^2. Dozens of paleo-shorelines are visible around Paiku Co. The highest paleo-shoreline is ~80 m above the modern lake level. Wünnemann et al. (2015) found that there was a close relationship between glacier dynamics and lake-level changes since the Last Glacial Maximum (LGM). The lake has been shrinking since the 1970s (Nie et al., 2013; Dai et al., 2013). Between 1972 and 2015, lake levels at Paiku Co decreased by 3.7 ±0.3 m and water storage reduced
85 by 8.5 % (Lei et al., 2018). According to rain gauge data collected between 2013 and 2016, annual rainfall in Paiku Co basin fluctuated significantly year to year. Typical annual precipitation varied between 150~200 mm, indicating that the lake basin belongs to the dry belt in the northern slope of Himalaya mountains (Wang et al., 2019). The mean annual temperature was 4.4^{o}C between June 2015 and May 2016 (Lei et al., 2018).

2.2 Data acquisition

90 In-situ observations, including lake water temperature, hydrometeorology, lake level and runoff, were carried out in Paiku Co basin. HOBO water-temperature loggers (U22-001, Onset Corp., USA) were used to monitor water temperature with an accuracy of ±0.2 ^{o}C. Two water-temperature profiles were set up in Paiku Co's southern (0-42 m in depth) and northern (0-72 m in depth) basins (Fig. 1). In the southern basin, water temperature was monitored at the depths of 0.4 m, 5m, 10 m, 15 m, 20 m, 30 m and 40 m. In the northern basin, water temperature was monitored at the depths of 0.4 m, 10 m, 20 m, 40 m,
95 50 m, 60 m and 70 m. Since lake level fluctuates seasonally, the depth of water temperature loggers may also have fluctuated

in a range of 0.4-0.8 m. Water temperatures were recorded at an interval of 1 hour and daily values were used to investigate thermal structure of the lake and estimate changes in lake heat storage. Three years' observational data from June 2015 to May 2018 from the southern basin was acquired, while only one year's data (June 2016 and May 2017) from the northern basin was acquired.

100 >>Fig. 1<<

Air temperature and relative humidity above the shoreline were monitored since June 2015 using HOBO air-temperature and humidity loggers (U12-012, Onset Corp., USA). The instrument has an accuracy of 0.35 ^{o}C for air temperature and 2.5% for relative humidity. Two loggers were installed in an outcrop ~2 m above the lake surface. One is located in the north shoreline of Paiku Co, the other is located in the central shoreline of Paiku Co (Fig. 1). The instruments were under large

105 rock where there was a hole facing the lake. The monitoring site was ventilated and therefore the meteorological condition over the lake surface can be recorded. Air temperature and relative humidity were recorded at an interval of 1 hour and daily values were used to estimate Bowen ratio. The air temperature and humidity measurements in the shoreline were further validated by a simple AWS (GMX 600) in the Paiku Co's southern center (Section 3.6). There was no data available between February and May 2017 because the instrument battery was too low.

110 Radiation, including downward shortwave radiation and longwave radiation to lake, was measured by Automatic Weather Station (AWS) at Qomolangma station for Atmospheric Environmental Observation and Research, Chinese Academy of Sciences (CAS). This station (87 °1.22′E, 28 °25.23′N, 4276 m a.s.l) is located at the northern slope of Mount Everest, about 150 km east of Paiku Co. The 2 m air temperature, relative humidity, wind speed and radiation were recorded at an interval of 10 min. In this study, daily solar radiation and downward longwave radiation at this station were used to calculate the net

115 radiation over the lake surface. The climate conditions between Paiku Co and Qomolangma station were similar, including topography, altitude, precipitation etc. The related information about hydrometeorology observations in Paiku Co basin are listed in Table 1.

As an important part of lake water budget, runoff was measured at three main rivers, i.e. Daqu, Bulaqu and Barixiongqu (Fig. 1). The water level of the three rivers was recorded automatically at an interval of 1 hour by using HOBO water-level

120 loggers (U20-001-01). Runoff during the pre-monsoon and post-monsoon seasons was measured at least twice a day, including the largest runoff in the afternoon and lowest runoff in the morning during field expedition using a LS1206B propeller-driven current meter (Nanjing Institute of Hydrological Automatization). Meanwhile, lake level was recorded at an interval of 1 hour in the littoral zone of north Paiku Co (Lei et al., 2018). Daily water levels of Paiku Co and its rivers were used to compare with the seasonal pattern of lake evaporation.

125 **2.3 Energy budget derived lake evaporation**

Lake evaporation was calculated using energy budget (Bowen-ratio) method, which has been described by Winter et al. (2003) and Rosenberry et al. (2007). The energy budget of a lake can be mathematically expressed as:

$$R = H + lE + S + G + A_v \quad (1)$$

where R is the net radiation over the lake, H is the sensible heat flux from lake surface, lE is the latent heat utilized for evaporation, S is change in lake heat storage, G is the heat transfer between lake water and bottom sediment, and A_V is the energy advected into lake water. The units used for the terms of Eq (1) are W·m^{-2}.

Av can be roughly estimated using total river discharge and the water temperature difference between river and lake. Lake water temperature was similar to that of river between April and June, but 2-6°C higher between July and December (Fig. S3). As a deep lake, total river discharge to Paiku Co was about 800-1000 mm water equivalent to lake level, accounting for 2-2.5% of total lake storage. The river discharge can accumulatively decrease lake water temperature by ~0.1 °C in summer, which corresponds to 2.1 W·m^{-2} of heat flux between July and September and 0.07 mm/day of lake evaporation. Therefore, the impact of river discharge and precipitation on the energy budget at Paiku Co is relatively small and can be neglected. Meanwhile, the heat transfer between lake water and bottom sediment (G) is also neglected because groundwater discharge is usually considered to be much less than surface runoff and geothermal is not detected at the lake bottom of Paiku Co.

The net radiation on the lake can be expressed as the following:

$$R = R_s - R_{sr} + R_l - R_{lr} - R_w \quad (2)$$

where R_s is solar radiation, R_{sr} is the reflection of solar radiation from lake surface, which is taken as 0.07 R_s (Gianniou and Antonopouls, 2007), R_l is atmospheric longwave radiation to lake, R_{lr} is the reflected longwave radiation from the lake surface, which is taken as 0.03 R_l, and R_w is the upward longwave radiation from lake. The units of the items in Eq (2) are W·m^{-2}.

The upward longwave radiation from lake (R_w) is approached by the equation:

$$R_w = \varepsilon_a \times \sigma \times (T_w + 273.15)^4 \quad (3)$$

where σ is the Stefan-Boltzmann constant (=5.67×10^{-8} W·m^{-2}·K^{-4}), ε_a is the water emissivity (0.97 for water surface) and T_w is lake surface temperature (°C). In this study, the water temperature at the depth of 0.4-0.8 m was used to represent the lake surface temperature. Note that the bulk temperature is slightly different from the 'skin' temperature (Wilson et al., 2013; Prats et al., 2018; Sugita et al., 2020). There exists surface warming during the day and surface cooling at night for high elevation lakes. However, the daily difference between them is small during most time of a year because surface water can be mixed quickly by water convection or strong wind in the afternoon and the two uncertainties by surface warming and cooling can cancel each other on daily timescale.

The sensible heat flux is related to the evaporative heat flux through the Bowen ratio (Henderson-Sellers, 1984):

$$\beta = \frac{H}{lE} = \gamma \times P \times \frac{T_w - T_a}{e_{sw} - e_d} \quad (4)$$

where β is Bowen ratio, T_w is lake surface temperature (°C), T_a is air temperature (°C) at 2m high above the water surface, e_{sw} and e_d are the saturated vapour pressure (kPa) at the temperature of the water surface and the air vapour pressure (kPa) above the water surface, respectively, P is air pressure (kPa), and γ is the psychrometric constant, 6.5×10^{-4} °C^{-1}. Air temperature, air pressure and specific humidity were monitored at the lake's shore. Saturated vapour pressure at the lake

surface was calculated according to the lake water temperature at the depth of 0.4-0.8 m in the lake centre. Daily Bowen ratio is calculated in this study.

Changes in lake heat storage (S) were calculated according to the detailed lake bathymetry and water temperature profile:

$$S = \frac{\sum_{i=0}^{15} c_w \times \rho_w \times \Delta V_i \times \Delta T_i}{A_l} \quad (5)$$

165 where c_w is the specific heat of water (J·kg^{-1}·K^{-1}), ρ_w is water density (=1000 kg·m^{-3}), ΔV_i is the lake volume at certain depth (m^3), and ΔT_i is water temperature change at the same depth, A_l is lake area (m^2). Changes in lake heat storage were calculated at an interval of 5 m and therefore there are 15 layers in vertical direction (the maximum depth: 72.8 m). ΔV_i was acquired according to the 5 m isobath of Paiku Co (Lei et al., 2018). ΔT_i was calculated at 5 m interval as the average temperature of the top and bottom layer. Changes in lake heat storage for the bottom water (>40 m) in 2015/2016 and

170 2016/2017 were calculated according to the data in 2016/2017 since there is no data available in the other two years. Lake heat storage, sensible and latent heat fluxes and lake evaporation were calculated at weekly interval in order to reduce their uncertainty caused by the spatial difference of solar radiation and lake water temperature.

3 Results and discussion

3.1 Thermal regime

175 Water temperature profiles between 2015 and 2018 show that Paiku Co was thermally stratified between July and October, and fully mixed between November and June in each year of the study period (Fig. 2). Lake water temperature increased rapidly from 2 to 7 $^{\circ}$C between April and June due to the high solar radiation. During this warming period, water temperature between the lake surface and bottom was almost same, indicating the lake water was well mixed. The vertical temperature gradient increased considerably in late June and clear stratification occurred by July. The occurrence of thermal stratification

180 corresponded to a significant reduction in wind speed. Wind speed was relatively low between July and the middle of October, and high in other months (Fig. S2). Strong lake surface heating and a reduction in wind speed together contributed to the development of thermal stratification (Wetzel, 2001). During the summer stratification period, the surface water warmed rapidly from 7 to ~13 $^{\circ}$C between July and August, while the bottom water warmed much more slowly. As a result, surface water reached its highest temperature in late August while bottom water (>40 m) reached to its highest temperature

185 by middle to late October. The thermocline formed between 15 m and 25 m water depth, with the largest temperature difference of 5~6 $^{\circ}$C in late August.

Lake surface temperature started to decrease gradually since September due to reduced solar radiation, while the bottom water continued to warm slowly (Fig. 2). As a result, the vertical temperature gradient decreased gradually. The lake stratification totally broke down in late October of each year, corresponding to significantly increased wind speed during this

190 period (Fig. S2). Notably, the breakdown of stratification occurred gradually, with the mixed layer deepening throughout October (Fig. 2). The mixed layer reached 40 m water depth on 13 October, and to 70 m water depth about two weeks later

(30 October). Following the complete breakdown of the water column's stratification, the bottom water experienced rapid warming over several days due to its mixing with the warmer water from the upper layer. For example, the water temperature at 70 m water depth remained stable at ~6.9 $^{\circ}$C from July to October, but increased abruptly from 6.9 to 8.6 $^{\circ}$C over several days (25 October to 30 October). Paiku Co's water column was fully mixed by November as indicated by the identical lake water temperature profiles at the two monitoring sites (Fig. 2, 3). Water temperature of the whole lake decreased gradually from 8.6 to 1 $^{\circ}$C from November to January and remained stable at 1-2 $^{\circ}$C until March.

These changes in thermal structure indicate that Paiku Co is a dimictic lake, which is similar to Bangong Co (Wang et al., 2014) and Nam Co (Wang et al., 2019), but different from Dagze Co (Wang et al., 2014). The vertical temperature gradients of Paiku Co (also including other lakes on the TP) are considerably lower compared with those in other parts of the world, for example Lake Qiaodaohu (area: 580 km^2, maximum depth: 108 m) in east China (Zhang et al., 2014), Lake Zurich (area: 65 km^2, maximum depth: 136 m) on the Swiss Plateau (Livingstone, 2003) and Lake Simcoe (area: 580 km^2, maximum depth: >40 m) in Canada (Stainsby et al., 2011). This may be mainly related to the high elevation of Paiku Co. Due to the elevation effect, the highest air temperature in Paiku Co basin is only ~12 $^{\circ}$C in summer and the highest lake surface temperature is 13 $^{\circ}$C, which is considerably lower than those in other parts of the world (e.g. Lake Qiaodaohu: ~32 $^{\circ}$C, Lake Zurich: ~22 $^{\circ}$C and Lake Simcoe: ~22 $^{\circ}$C), while the bottom water temperature does not show much difference with these lakes (e.g. Paiku Co: 7 $^{\circ}$C, Lake Qiaodaohu: ~10 $^{\circ}$C, Lake Zurich: ~5 $^{\circ}$C, and Lake Simcoe: ~4 $^{\circ}$C).

>>Fig. 2<<

>>Fig. 3<<

3.2 Energy budget over the lake surface

The main components of energy budget over the lake surface, including solar radiation, atmospheric longwave radiation to the lake and upward longwave radiation from the lake body, are shown in Fig. 4a-c. Solar radiation had an annual average of 251.8 W·m^{-2} (Fig. 4), which is slightly higher than the TP average due to its lower latitude (Yang et al., 2010). Atmospheric longwave radiation and upward longwave radiation from the lake body had an annual average of 235.8 W·m^{-2} and 336.8 W·m^{-2}, respectively. The net radiation over Paiku Co varied seasonally in a range of 19.0~212.1 W·m^{-2}, with an average value of 125.8 W·m^{-2}. Relatively high net radiation occurred from April to August, with the highest value of 212.1 W·m^{-2} in June. Relatively low net radiation occurred from October to February, with the lowest value of 19.7 W·m^{-2} in December.

>>Fig. 4<<

Changes in heat storage at Paiku Co were quantified using in-situ observations of water temperature profiles and detailed lake bathymetry (Fig. 4e), which makes it possible to evaluate the impact of lake heat storage on the heat flux over the lake surface. Between April and July, when Paiku Co warmed gradually, the lake water absorbed energy at an average rate of 128.6 W·m^{-2}, accounting for 66.5% of the net radiation during the same period. The lake heat storage increased most rapidly in June, with an average rate of 191.6 W·m^{-2}, accounting for 91.6% of the net radiation during the same period. The lake heat

storage reached its peak in late August, when the surface water temperature was highest. Between October and January,
when the lake water cooled, the lake released energy to the overlying atmosphere at an average rate of 137.5 W·m^{-2}, which
was more than 3 times greater than the net radiation during the same period. The lake heat storage decreased most rapidly in
November at an average rate of 193.6 W·m^{-2}, which was about 5 times greater than the net radiation during the same period.
The Bowen ratio varied in a range of -0.26~+0.37 (Fig. 5c). Negative values occurred between April and July, with an
average value of -0.12. Positive values occurred between August and December, with an average value of +0.20. Latent heat
flux was the main component of the total heat flux with an average value of 112.3 W·m^{-2} between May and December.
Latent heat flux was low between May and June with an average of 38.7 W·m^{-2} and was high between October and
December with an average of 153.3 W·m^{-2} (Tab. 2). Latent heat flux at Paiku Co was positively correlated with the water
vapour pressure difference between the lake surface and the overlying atmosphere (r^2=0.41, P<0.001). Sensible heat flux had
an average value of 13.3 W·m^{-2} between May and December, accounting for ~11% of latent heat flux. Sensible heat flux was
negative between April and July with an average value of -5.6 W·m^{-2} and was in positive value between August and
December with an average of 23.0 W·m^{-2} (Tab.2). The sensible heat flux was positively correlated with the water
temperature difference between surface water and the overlying atmosphere (r^2=0.86, P<0.001).

>>Fig. 5<<

3.3 Lake evaporation

Lake evaporation at Paiku Co between May and December was determined using energy budget method (Fig. 6). Lake
evaporation between January and April was not determined because part of the lake surface was covered by lake ice which
can significantly affect the energy balance over the lake surface. Lake evaporation was generally low during the pre-
monsoon season (May and Jun) with an average value of 1.7 mm/day. During the monsoon season (Jul to Sep), lake
evaporation increased rapidly from 2.9 to 5.1 mm/day. High lake evaporation occurred during the post-monsoon season (Oct
to Dec), with an average value of 5.4 mm/day. The total lake evaporation was estimated to be 975 mm during the entire ice-
free period between May and December.

>>Fig. 6<<

Lake evaporation at Paiku Co exhibited a similar seasonal pattern with changes in lake heat storage due to large lake heat
storage. There is ~5 months lag between the maximum lake evaporation and maximum net radiation at Paiku Co. Regression
analysis shows that lake evaporation at Paiku Co was positively correlated with changes in lake heat storage (r^2=0.63), but
negatively correlated with net radiation (r^2=0.22), which indicates that the seasonal pattern of lake evaporation was
significantly affected by lake heat storage. When the net radiation was high between May and July, most of the energy was
used to heat the lake water and only a small part of it was consumed as the latent heat flux, which led to low lake evaporation.
When the net radiation was low between October and December, a large amount of heat was released from the lake water as

255   latent heat to the overlying atmosphere, which led to high lake evaporation. Lake evaporation exhibited similar patterns with the water vapour pressure difference between surface water and the overlying atmosphere (r^2=0.33).

3.4 Impact of lake heat storage on the seasonal pattern of lake evaporation

To further explore the impact of lake heat storage on the seasonal pattern of lake evaporation, we compare lake evaporation at Paiku Co with other lakes on the TP. We only select lakes with eddy covariance system measurements. At Ngoring Lake

260   (area, 610 km^2; mean depth, 17 m) on the eastern TP, Z. Li et al. (2015) investigated the lake's energy budget and evaporation in 2011-2012, and found that the latent heat at Nogring Lake was lowest in June, peaked in August and then decreased gradually from September to November. At Qinghai Lake (area, 4430 km^2; mean depth, 19 m) on the northeast TP, X. Li et al. (2016) conducted studies concerning the lake's energy budget and evaporation in 2013-2015, and found that there was a 2–3 month delay between the maximum net radiation and maximum heat flux. Compared with Paiku Co, there was

265   shorter time lag between the heat flux and net radiation at the two relatively shallow lakes. The different phase of lake evaporation among these lakes can be partly attributed to lake heat storage. As we have shown, Paiku Co has a mean water depth of ~41 m and the water column is fully mixed between November and June. This means that Paiku Co as a deep lake can store more energy during the pre-monsoon and monsoon season than relatively shallow lakes, and subsequently release more energy to the overlying atmosphere during the post-monsoon season.

270   At Nam Co, a large and deep lake on the central TP, there have been several studies regarding lake evaporation (Haginoya et al., 2009; Ma et al., 2016; Wang et al., 2017, 2019). Haginoya et al. (2009) found that lake evaporation at Nam Co was lowest in May and highest in October. Lake evaporation at Nam Co was estimated to be 916~986 mm through Bowen ratio method (Lazhu et al. 2016) and eddy covariance system (Wang et al., 2019). Fig. 6 shows that lake evaporation at Paiku Co and Nam Co exhibits similar seasonal variations. In fact, although the maximum depth at Nam Co is greater than that at

275   Paiku Co, the average water depth of the two lakes is similar (Wang et al., 2009; Lei et al., 2018), which results in a similar seasonal pattern of changes in lake heat storage and lake evaporation (Fig. 6). At Siling Co, another large lake on the central TP, monthly lake evaporation varied within a range of 2.4-3.3 mm/day between May and September, 2014, with a total amount of 417.0 mm during the study period (Guo et al., 2016). Although the cumulative evaporation between Paiku Co and Siling Co is similar between May and September, lake evaporation during the post-monsoon season cannot be further

280   compared because the energy flux at Siling Co was not measured.

3.5 Implications for the seasonal lake-level variations across the TP

The quantification of lake evaporation is important for understanding lake water budget and associated lake-level changes. Compared with the eddy covariance system that can only work until October/November when the lake surface begins to freeze (Li et al., 2015; Wang et al., 2017; Guo et al., 2016), our results give a full description of lake evaporation during the

285   entire ice-free period. More importantly, our results indicate that for deep lakes on the TP, evaporation during the post-monsoon season can be much higher than that during the pre-monsoon season due to the release of large amount of stored

heat, despite both air temperature and net radiation are already low. In this sense, lake evaporation during the post-monsoon season is of great importance to lake water budget and can significantly affect the amplitude of seasonal lake-level changes, especially for deep lakes.

290 As a monsoon dominated region, Indian summer monsoon around Paiku Co usually started in middle June and ended in late September (Yu et al., 2016). For most years, more than 80% precipitation occurred during the summer monsoon season. Glacier melting also occurred during the summer monsoon season. In contrast, heat flux at Paiku Co was low during the pre-monsoon and monsoon seasons and high during the post-monsoon season. This contrasting pattern of hydrological and thermal intensities played an important role in the large amplitude of seasonal lake-level changes at Paiku Co. Precipitation

295 and lake inflow, for instance, were mainly concentrated during the monsoon season, while lake evaporation was still low during this period (Fig. 7a-b), which caused a positive lake water budget and a rapid increase in lake level (40~60 cm). During the post-monsoon season, precipitation and lake inflow were already very low, while lake evaporation was high, which led to a negative lake water budget and a rapid decrease in lake level (~40 cm). A slight lake-level decrease occurred during the pre-monsoon season due to low lake evaporation and lake inflow.

300 >>Fig. 7<<

On a broader scale, lake evaporation may affect the different amplitude of seasonal lake-level variations between deep and shallow lakes on the TP. Lei et al (2017) investigated the lake-level seasonality across the TP and found that there were different amplitudes of seasonal lake-level fluctuations even in similar climate regimes. For example, lake level at Nam Co and Zhari Namco, two large and deep lakes on the central TP (Wang et al., 2009, 2010), decreased considerably by 0.3-0.5 m

305 during the post-monsoon season (Fig. 8), while lake level at two nearby small lakes, Bam Co and Dawa Co, decreased slightly by 0.1-0.2 m during the same period. Different seasonal pattern of lake evaporation may play an important role in the amplitude of lake-level seasonality. For deep lakes (e.g. Paiku Co, Nam Co and Zhari Namco), the latent heat flux (lake evaporation) over lake surface may lag the solar radiation by several months due to the large heat storage. For this kind of lake, the lake-level drop mainly occurs during the post-monsoon season when lake evaporation is high but lake water input is

310 low. For shallow lakes, the latent heat flux closely follows solar radiation due to small lake heat storage, namely high lake evaporation occurs during the pre-monsoon and monsoon seasons, and low lake evaporation occurs during the post-monsoon season (Morrill et al., 2004). Meanwhile, shallow lakes freeze up 1-2 months earlier than deep lakes. When the lake surface is covered by ice, lake evaporation (sublimation) is significantly reduced (Huang et al., 2019). Consequently, lake level at shallow lakes decreased slowly during the post-monsoon season than that at deep lakes. This phenomenon can also be seen

315 in some thermokarst lakes on the northern TP (Luo et al., 2015; Pan et al., 2017).

Lake evaporation may also have significant impact on the different amplitude of seasonal lake-level variations between the northern and southern TP. Based on ICESat satellite altimetry data, Phan et al (2012) showed that there was a larger amplitude of seasonal lake-level variations on the southern TP relative to the northern TP. However, the main causes have not been investigated until now. Generally, it is much colder on the northern TP than the southern TP due to elevation and

320 latitude effects (Maussion et al., 2014). Lakes on the northern TP usually freeze up earlier and break up later relative to the

southern TP (Kropacek et al., 2013), which results in longer ice cover duration on the northern TP (159-209 days) relative to the southern TP (126 days). Longer ice cover duration on the northern TP can considerably reduce lake evaporation during the post-monsoon season (Wang et al., 2020). Meanwhile, lakes on the southern TP are usually larger and deeper than those on the northern TP (e.g. Wang et al., 2009, 2010), which indicates that it can store more energy during the pre-monsoon and monsoon seasons, and release it to the overlying atmosphere during the post-monsoon season. For endorheic lakes, relatively higher lake evaporation during the post-monsoon season may lead to larger lake-level decrease on the southern TP compared with the northern TP. Therefore, the different amplitudes of seasonal lake-level variations between the southern and northern TP can be partly attributed to the different seasonal pattern of lake evaporation. Note that besides lake ice phenology other factors including lake salinity and solar radiation may also have impact on the spatial difference of lake evaporation on the TP. More studies are still needed to quantify their impact on annual lake evaporation and the seasonal distribution.

\>>Fig. 8<<

3.6 Uncertainty of lake evaporation

Uncertainty of lake evaporation can be mainly caused by the following factors: solar radiation, lake surface temperature, changes in lake heat storage, meteorological data (air temperature and humidity).

Firstly, solar radiation and atmospheric longwave radiation at Qomolangma station were used to represent those at Paiku Co. To evaluate the spatial difference, we made a comparison of solar radiation at Paiku Co and Qomolangma Station by using Hamawari-8 satellite data (Fig. S4; Tang et al., 2019). The results show that daily solar radiation at the two sites exhibited similar seasonal fluctuations (R^2=0.55, P<0.001). The mean difference of solar radiation at the two sites was estimated to be 3.8 W·m^{-2} (ΔE_1). The uncertainty in the atmospheric longwave radiation is not estimated, but the variations of solar radiation and atmospheric longwave radiation are usually opposite at a site, so their total uncertainty should not exceed the individual uncertainty.

Secondly, lake water temperature at the depth of 0.4-0.8 m, not lake skin temperature is used to calculate upward longwave radiation. Studies show that lake skin temperature is higher than surface water temperature at daytime, and vice versa at nighttime (Prats et al., 2018). Here Aqua MODIS 8-day lake surface temperature product is used to determine the difference between lake bulk temperature and skin temperature. The product is produced with spatial resolution of about 1 km and the accuracy is estimated to be 1 K under clear sky conditions (Wan, 2013). During the pre-monsoon and monsoon seasons when the lake water gets warm, the skin temperature derived from MODIS data is about 1.2 ^{o}C higher than lake body temperature. During the post-monsoon season when the lake water gets cool, the skin temperature derived from MODIS data is about 0.05 ^{o}C higher than lake body temperature. Because MODIS data is easily affected by cloud cover and other factors during the monsoon season, the mean difference of 0.05 ^{o}C during the post-monsoon season is used to estimate uncertainty of upward longwave radiation, which is estimated to be 7.6 W·m^{-2} (ΔE_2) by using error propagation.

Thirdly, uncertainty of changes in lake heat storage mainly comes from the spatial distribution of lake water temperature. A comparison of lake water temperature between Paiku Co's southern and northern basins in 2016/2017 was shown in Fig. S5.

Since the northern basin is much deeper than the southern basin, lake water in the northern basin warmed more slowly than that in the southern basin during the pre-monsoon and monsoon seasons, and cooled more slowly during the post-monsoon. The daily surface water temperature in the southern basin was about 0.85 $^{\circ}$C higher on average than that in the northern basin between April and September, but was about 0.45 $^{\circ}$C lower on average in November and December (Fig. S5). Water temperature became spatially uniform at both basins between January and March. Similar spatial difference can also be found at 10 m depth, indicating that this phenomenon may exist in the entire epilimnion. Uncertainty of changes in lake water temperature is estimated to be 0.007 $^{\circ}$C/day during the ice-free period, corresponding to 14.3 W·m^{-2} of changes in lake heat storage (ΔE_3).

Fourthly, air temperature and relative humidity at the shoreline are used to calculate Bowen ratio and lake evaporation. To validate its representativeness, we set up a platform (water depth: 19 m; least distance from shoreline: 2 km) in the southern centre of Paiku Co in September 2019 and a simple AWS station (GMX600) was installed on the platform. Meteorological data between 22 September and 26 October were acquired. We made a comparison of meteorological data between shoreline and lake centre. Results show that both air temperature and relative humidity fluctuated similarly between the shoreline and lake centre (Fig. 9), indicating the meteorological data from the shoreline of Paiku Co can be used to represent the general condition of the whole lake at least during the observed period. The RMSE of daily air temperature and water vapour pressure in the shoreline was estimated to be 0.91 $^{\circ}$C and 0.069 kPa. The uncertainty of Bowen ratio was estimated to be 0.02 during the ice-free period by using error propagation, which corresponds to 2.2 W·m^{-2} of heat flux (ΔE_4). By using error propagation, the uncertainties of latent heat flux and lake evaporation are estimated to be 16.8 Wm^{-2} ($= \sqrt{{\Delta E_1}^2 + {\Delta E_2}^2 + {\Delta E_3}^2 + {\Delta E_4}^2}$) and 0.6 mm/day, corresponding to 142 mm of the total uncertainty of lake evaporation.

>>Fig. 9<<

Lake evaporation is validated by comparing with lake-level changes during the pre-monsoon and post-monsoon seasons. Runoff measurements at the three largest rivers feeding Paiku Co are shown in Tab. 3. During the pre-monsoon season (May), lake evaporation (1.7 mm/day) was similar with the rate of lake-level decrease (1.8 mm/day). During the post-monsoon season (Oct to Dec), lake evaporation (5.4 mm/day) was considerably higher than the rate of lake-level decrease (3.8 mm/day). This discrepancy (1.6 mm/day) may be partly due to the contribution of precipitation and surface runoff. As shown in Table 3, runoff at the three large rivers can contribute to lake-level increase by 1.0 mm/day on average in October, thereby partially offsetting lake-level changes from lake evaporation. This difference (0.6 mm/day) between the estimated lake evaporation and the in-situ measurements of lake-level decrease and runoff during the post-monsoon season is very close to the uncertainty of lake evaporation estimated by error propagation.

4 Conclusion

Lake evaporation and its effects on seasonal lake-level variations at Paiku Co on the southern TP were investigated based on three years' comprehensive observations of lake water budget, including hydrometeorology, water temperature profile, lake level and runoff etc. The results show that Paiku Co is a dimictic lake with clear lake stratification between July and October. The surface water reached its highest temperature in late August while the bottom water reached its highest two months later. The thermocline formed at the depth of 15~25 m, with the largest temperature difference of 5~6 $^{\circ}$C in late August.

As a deep alpine lake, the seasonal patterns of heat flux and lake evaporation are significantly affected by the large lake heat storage. The lake absorbed most of net radiation to heat the lake water during the pre-monsoon and monsoon season and released it to the overlying atmosphere during the post-monsoon season. Between April and July, about 66.5% of the net radiation was consumed to heat the lake water. Between October and January, heat released from lake water was about 3 times larger than the net radiation. As a result, there was ~5 months lag between the maximum lake evaporation and the maximum net radiation due to the large heat storage of lake water. Lake evaporation at Paiku Co was estimated to be 975±142 mm during the ice-free period between May and December, with low values of 1.7±0.6 mm/day during the pre-monsoon season (May and Jun), and high values of 5.4±0.6 mm/day during the post-monsoon season (Oct to Dec).

Our results imply that lake evaporation played an important role in the different amplitudes of seasonal lake-level variations on the TP. For deep lakes like Paiku Co, contrasting hydrological and thermal intensities determines the large amplitude of seasonal lake-level variations. High lake evaporation and low lake inflow lead to the considerable lake-level decrease during the post-monsoon season. In contrast, relatively low lake evaporation but high lake inflow led to rapid lake-level increase during the monsoon season (Jun to Aug). For relatively shallow lakes, the seasonal pattern of lake evaporation varies similarly with the net solar radiation, which results in slight lake-level decrease during the post-monsoon season and less amplitude of lake-level seasonality. Our results may have further implication for the different amplitudes of seasonal lake-level variation between deep and shallow lakes and between the southern and northern TP.

Data availability

All original data presented in this paper are publicly available via National Tibetan Plateau Data Center (http://data.tpdc.ac.cn/en/).

Author contribution

Lei Y.B. and Yao T.D. conceived and designed the experiments; Lei. Y.B., Yao T.D., Yang K., Lazhu, and Ma Y.M. analyzed the data; Lei Y.B. performed the fieldwork and wrote the paper; Bird B.W. helped write the paper.

Competing interests

The authors declare that they have no conflict of interest.

Acknowledgement

415 This research has been supported by the Second Tibetan Plateau Scientific Expedition and Research Program (2019QZKK0201), the Strategic Priority Research Program of Chinese Academy of Sciences (XDA2006020102), the NSFC project (41971097 and 21661132003) and Youth Innovation Promotion Association CAS (2017099). We thank Qomolangma Atmospheric and Environmental Observation and Research Station CAS for providing radiation data, Dr. Wenjun Tang for providing Hamawari-8 satellite radiation data. We are also grateful to all the members who took part in the

420 fieldwork.

References

Blanken, P. D., Rouse, W. R., Culf, A.D., Spence, C., Boudreau, L.D., Jasper, J.N., Kochtubajda, B., Schertzer, W. M., Marsh, P., and Verseghy, D.: Eddy covariance measurements of evaporation from Great Slave Lake, Northwest Territories, Canada, Water Resour. Res., 36, 1069–1078, 2000.

425 Cai, Y., Ke, C. Q., and Duan, Z.: Monitoring ice variations in Qinghai Lake from 1979 to 2016 using passive microwave remote sensing data. Sci. Total Environ., 607–608, 120-131, doi:425 10.1016/j.scitotenv.2017.07.027, 2017.

Dai, Y., Gao, Y., Zhang, G., and Xiang, Y.: Water volume change of the Paiku Co in the southern Tibetan Plateau and its response to climate change in 2003–2011, J. Glaciol. Geocryol., 35 (3), 723–732, 2013.

Gianniou, S. K., and Antonopoulos V. Z.: Evaporation and energy budget in Lake Vegoritis. Greece, J. Hydrol., 345, 212–

430 223, 2007.

Guo, Y., Zhang, Y., Ma, N., Song, H., Gao, H.: Quantifying Surface Energy Fluxes and Evaporation over a significant Expanding Endorheic Lake in the Central Tibetan Plateau, J. Meteorol. Soc. Jpn., 94, 453–465, 2016.

Haginoya, S., Fujii H., Kuwagata T., Xu J., Ishigooka Y., Kang S., and Zhang Y.: Air-lake interaction features found in heat and water exchanges over Nam Co on the Tibetan Plateau, Sci. Online Lett. Atmos., 5, 172–175, doi:10.2151/sola.2009-044,

435 2009.

Henderson-Sellers, B. Engineering Limnology. Pitman Publishing, Great Britain. 1984.

Huang, W., Cheng, B., Zhang, J., Zhang, Z., Vihma, T., Li, Z., Niu, F.: Modeling experiments on seasonal lake ice mass and energy balance in the Qinghai-Tibet Plateau: a case study, Hydrol. Earth Syst. Sci. 23, 2173–3186, 2019.

Ke, C., Tao, A., Jin, X.: Variability in the ice phenology of Nam Co Lake in central Tibet from scanning multichannel

440 microwave radiometer and special sensor microwave/imager: 1978 to 2013. J. Appl. Remote. Sens. 7, 073477. http://dx.doi.org/10. 1117/1.JRS.7.073477, 2013.

Kropacek, J., Maussion, F., Chen, F., Hoerz, S., Hochschild, V.: Analysis of ice phenology of lakes on the Tibetan Plateau from MODIS data. Cryosphere, 7 (1), 287–301. http://dx.doi.org/10.5194/tc-7-287-2013, 2013.

Lazhu, Yang, K., Wang, J., Lei, Y., Chen, Y., Zhu, L., Ding, B., and Qin, J.: Quantifying evaporation and its decadal change for Lake Nam Co, central Tibetan Plateau, J. Geophys. Res. Atmos., 121, doi:10.1002/2015JD024523, 2016.

Lei, Y., Yang, K., Wang, B., Sheng, Y., Bird, B., Zhang, G., and Tian, L.: Response of inland lake dynamics over the 405 Tibetan Plateau to climate change, Clim. Change, 125, 281–290, 2014.

Lei, Y., Yao, T., Yang, K., Sheng, Y., Kleinherenbrink, M., Yi, S., Bird, B.W., Zhang, X., Lazhu, Zhang, G.Q.: Lake seasonality across the Tibetan Plateau and their varying relationship with regional mass changes and local hydrology, Geophys. Res. Lett., 44, doi:10.1002/2016GL072062, 2017.

Lei Y., and Yang K.: The cause of rapid lake expansion in the Tibetan Plateau: climate wetting or warming? WIREs Water, e1236. DOI:10.1002/wat2.1236, 2017.

Lei, Y., Yao, T., Yang, K., Bird B.W., Tian, L., Zhang, X., Wang W., Xiang Y., Dai, Y.F., Lazhu, Zhou, J., Wang, L.: An integrated investigation of lake storage and water level changes in the Paiku Co basin, central Himalayas, J. Hydrol., 562, 599–608, doi.org/10.1016/j.jhydrol.2018.05.040, 2018.

Lenters, J., Kratz, T., and Bowser, C.: Effects of climate variability on lake evaporation: results from a long-term energy budget study of Sparkling Lake, northern Wisconsin (USA), J. Hydrol., 308, 168–195, 2005.

Li, W., Li, S., and Pu P.: Estimates of plateau lake evaporation: A case study of Zige Tangco, J. Lake Sci., 13(3): 227–232, 2001.

Li, X.Y., Ma Y.J., Huang Y.M., Hu X., Wu X.C., Wang P., Li G.Y., and Zhang S.Y.: Evaporation and surface energy budget over the largest high-altitude saline lake on the Qinghai-Tibet Plateau, J. Geophys. Res.Atmos., 121, 10,470–10,485, doi:10.1002/2016JD025027, 2016.

Li, Z., Lyu, S., Ao, Y., Wen, L., Zhao, L., and Wang S.: Long-term energy flux and radiation balance observations over Lake Ngoring, Tibetan Plateau. Atmos. Res., 155, 13–25, doi:10.1016/j.atmosres.2014.11.019, 2015.

Livingstone, D.: Impact of secular climate change on the thermal structure of a large temperate central European lake. Climatic Changes, 57, 205-225, 2003

Luo, J., Niu, F., Lin, Z., Liu, M., Yin, G. Thermokarst lake changes between 1969 and 2010 in the Beilu River Basin, Qinghai–Tibet Plateau, China. Sci. Bull. 60(5),556–564, 2015.

Ma, N., J. Szilagyi, Niu, G.Y., Zhang, Y., Zhang, T., Wang, B., and Wu, Y.: Evaporation variability of Nam Co Lake in the Tibetan Plateau and its role in recent rapid lake expansion, J. Hydrol., 537, 27–35, doi:10.1016/j.jhydrol.2016.03.030, 2016.

Ma, R., Yang, G., Duan, H., Jiang, J., Wang, S., Feng, X., Li, A., Kong, F., Xue, B., Wu, J., Li, S.: China's lakes at present: number, area and spatial distribution. Sci. China Earth Sci. 54(2), 283–289, 2011.

Maussion, F., Scherer, D., Mölg, T., Collier, E., Curio, J., and Finkelnburg, R.: Precipitation Seasonality and Variability over the Tibetan Plateau as Resolved by the High Asia Reanalysis, J. Climate, 27, 1910–1927, 2014.

475   Morrill, C.: The influence of Asian summer monsoon variability on the water balance of a Tibetan lake, J. Paleolimnol., 32, 273-286, 2004.

Nie, Y., Zhang, Y., Ding, M., Liu, L., Wang, Z.: Lake change and its implication in the vicinity of Mt. Qomolangma (Everest), central high Himalayas, 1970–2009, Environ. Earth Sci. 68, 251–265, 2013.

Pan, X., Yu, Q., You, Y., Chun, K.P., Shi, X., Li, Y.: Contribution of supra-permafrost discharge to thermokarst lake water
480   balances on the northeastern Qinghai-Tibet Plateau, J. Hydrol., 555, 621–630, 2017.

Phan, V. H., Lindenbergh, R., and Menenti, M.: ICESat derived elevation changes of Tibetan lakes between 2003 and 2009, Int. J. Appl. Earth Obs., 17, 12–22, 2012.

Prats, J., Reynaud, N,, Rebière, D., Peroux, T., Tormos, T., and Danis, P.A.: LakeSST: Lake Skin Surface Temperature in French inland water bodies for 1999-2016 from Landsat archives. Earth Syst. Sci. Data, 10, 727–743, 2018.

485   Rosenberry, D.O., Winter, T.C., Buso, D.C., and Likens, G. E.: Comparison of 15 evaporation methods applied to a small mountain lake in the northeastern USA, J. Hydrol., 340, 149–166, doi:10.1016/j.jhydrol.2007.03.018, 2007.

Rouse, W. R., Oswald, C. J., Binyamin, J., Blanken, P. D., Schertzer, W. M., and Spence, C.: Interannual and seasonal variability of the surface energy balance and temperature of central Great Slave Lake, J. Hydrometeor., 4, 720–730, 2003.

Rouse, W. R., Blanken, P. D., Bussières, N., Oswald, C.J., Schertzer, W.M., Spence, C., and Walker, A.E.: An Investigation
490   of the Thermal and Energy Balance Regimes of Great Slave and Great Bear Lakes, J. Hydrometeor., 9, 1318–1333., 2008.

Song, C., Huang, B., Ke, L., and Richards K.: Seasonal and abrupt changes in the water level of closed lakes on the Tibetan Plateau and implications for climate impacts, J. Hydrol., 514, 131–144, 2014.

Stainsby, E.A., Winter J.G., Jarjanazi, H., Paterson, A.M., Evans, D.O., Young, J.D.: Changes in the thermal stability of Lake Simcoe from 1980 to 2008. J. Great Lakes Res., 37, 55–62, 2011.

495   Su, D., Hu, X., Wen, L., Lyu, S., Gao, X., Zhao, L., Li, Z., Du, J., and Kirillin G.: Numerical study on the response of the largest lake in China to climate change. Hydrol. Earth Syst. Sci., 23, 2093–2109, https://doi.org/10.5194/hess-23-2093-2019, 2019.

Sugita, M., Ikura, H., Miyano, A., Yamamoto, K., and Wei Z.: Evaporation from Lake Kasumigaura: annual totals and variability in time and space. Hydrological Research Letters, 8(3), 103-107, 2014.

500   Sugita, M.: Spatial variability of the surface energy balance of Lake Kasumigaura and implications for flux measurements, Hydrological Sci. J., DOI:10.1080/02626667.2019.1701676, 2019.

Sugita, M., Ogawa, S., and Kawade, M.: Wind as a main driver of spatial variability of surface energy balance over a shallow 102 – km2 scale lake: Lake Kasumigaura, Japan. Water Resour. Res., 56, e2020WR027173. https://doi.org/10.1029/2020WR027173, 2020.

505   Tang, W., Li, J., Yang, K., Qin, J., Zhang, G., Wang, Y.: Dependence of remote sensing accuracy of global horizontal irradiance at different scales on satellite sampling frequency. Solar Energy, 193, 597-603, 2019.

Wan, Z.: Collection-6 MODIS land surface temperature products users' guide. ICESS, University of California, Santa Barbara. 2013.

Wang, B., Ma, Y., Ma, W., and Su, Z.: Physical controls on half-hourly, daily, and monthly turbulent flux and energy budget over a high-altitude small lake on the Tibetan Plateau, J. Geophys. Res. Atmos., 122, 2289–2303, doi:10.1002/2016JD026109, 2017.

Wang, B., Ma, Y., Wang, Y., Su, Z., Ma, W.: Significant differences exist in lake-atmosphere interactions and the evaporation rates of high-elevation small and large lakes, J. Hydrol., 573, 220–234, 2019.

Wang, B., Ma, Y., Su, Z., Wang, Y., Ma, W.: Quantifying the evaporation amounts of 75 high-elevation large dimictic lakes on the Tibetan Plateau. Sci. Adv. 6, eaay8558, 2020.

Wang, J., Zhu, L., Daut, G., Ju, J., Lin, X., Wang, Y., and Zhen, X.: Investigation of bathymetry and water quality of Lake Nam Co, the largest lake on the central Tibetan Plateau, China, Limnology, 10, 149–158, doi:10.1007/s10201-009-0266-8. 2009.

Wang, J., Peng, P., Ma, Q., Zhu, L.: Modern limnological features of Tangra Yumco and Zhari Namco, Tibetan Plateau, J. Lake Sci., 22 (4), 629–632, 2010.

Wang, J., Huang, L., Ju, J., Daut, G., Wang, Y., Ma, Q., Zhu, L., Haberzettl, T., Baade, J., Mäusbacher, R.: Spatial and temporal variations in water temperature in a high-altitude deep dimictic mountain lake (Nam Co), central Tibetan Plateau. J. Great Lakes Res. 45, 212–223, 2019.

Wang, M., Hou, J., Lei, Y.: Classification of Tibetan lakes based on variations in seasonal lake water temperature. Chin, Sci. Bull., DOI 10.1007/s11434-014-0588-8, 2014.

Wang, Y., Yang, K., Zhou, X., Wang, B., Chen, D., Lu, H., Lin, C., and Zhang, F.: The formation of a dry‑belt in the north side of central Himalaya Mountains. Geophys. Res. Lett., 46, 2993–3000. https://doi.org/10.1029/2018GL081061, 2019.

Wetzel, R.G.: Limnology: lake and river ecosystems. Elsevier, San Diego, 2001.

Wilson, R. C., Hook, S. J., Schneider, P., and Schladow, S. G.: Skin and bulk temperature difference at Lake Tahoe: A case study on lake skin effect, J. Geophys. Res. Atmos., 118, 10,332–10,346, doi:10.1002/jgrd.50786, 2013.

Winter, T., Buso, D., Rosenberry, D., Likens, G., Sturrock Jr., A., Mau, D.: Evaporation determined by the energy-budget method for Mirror Lake, New Hampshire, Limnol. Oceanogr. 48 (3), 995–1009, 2003.

Wünnemann, B., Yan, D., Ci, R.: Morphodynamics and lake level variations at Paiku Co, southern Tibetan Plateau, China, Geomorphology. 246: 489–501, 2015.

Xu, J., Yu, S., Liu, J., Haginoya, S., Ishigooka, Y., Kuwagata, T., Hara, M., and Yasunari T.: The implication of heat and water balance changes in a lake basin on the Tibetan Plateau. Hydrol. Res. Lett., 3, 1–5, 2009.

Yang, K., He, J., Tang, W., Qin, J., and Cheng, C.: On downward shortwave and longwave radiations over high altitude regions: Observation and modeling in the Tibetan Plateau, Agric. For. Meteorol., 150(1), 38-46, doi:10.1016/j.agrformet.2009.08.004, 2010

Yu, S., Liu, J., Xu, J., and Wang, H.: Evaporation and energy balance estimates over a large inland lake in the Tibet-Himalaya, Environ. Earth Sci., 64(4), 1169–1176, 2011.

Yu, W., Yao, T., Tian, L., Ma, Y., Wen, R., Devkota, L., Wang, W., Qu, D., Chhetri, T.B.: Short-term variability in the dates of the Indian monsoon onset and retreat on the southern and northern slopes of the central Himalayas as de-termined by precipitation stable isotopes. Clim. Dyn. 47, 159–172, 2016.

545 Zhang, G., Yao, T., Xie, H., Zhang, K., Zhu, F.: Lakes' state and abundance across the Tibetan Plateau, Chin. Sci. Bull. 59 (24), 3010–3021, 2014a.

Zhang, G., Yao, T., Xie, H., Qin, J., Ye, Q., Dai, Y., & Guo, R.: Estimating surface temperature changes of lakes in the Tibetan Plateau using MODIS LST data. Journal of Geophysical Research: Atmospheres, 119, 8552–8567. https://doi.org/10.1002/2014JD021615, 2014b.

550 Zhang, Q., and Liu, H.: Seasonal changes in physical processes controlling evaporation over inland water, J. Geophys. Res. Atmos., 119, 9779–9792, doi:10.1002/2014JD021797, 2014.

Zhang, Y., Wu, Z., Liu, M., He, J., Shi, K., Wang, M., and Yu, Z.: Thermal structure and response to long-term climatic changes in Lake Qiandaohu, a deep subtropical reservoir in China, Limnol. Oceanogr., 59(4), 1193–1202, 2014.

555

560

565

570

575

Figure and Captions

Table 1 The related information about hydro-meteorology observations

Parameter	Sensor	Accuracy	Location	Duration
T_w	HOBO U22-001	0.21 ^{o}C	South center	2015.6-2018.5
			North center	2016.6-2017.5
T_a and RH	HOBO U12-012	0.35 ^{o}C 2.5%	Shoreline	2015.6-2017.1, 2017.6-2018.5
T_a and RH	GMX600	0.3 ^{o}C 2%	South center	2019.9-2019.10
R_s and R_l	Kipp & Zonen CNR4 net radiometer	1%	Qomolangma Station, CAS	2015.6-2017.12

T_w=water temperature; T_a=air temperature; RH=relative humidity; R_s=shortwave solar radiation; R_l=downward long wave radiation

580

585

590

595

600

Table 2 Monthly net radiation, total lake heat storage, Bowen ratio and lake evaporation between 2015 and 2017

Month	Net energy (W·m^{-2})			Heat storage (W·m^{-2})			Bowen Ratio			Evaporation (mm/day)		
	2015	2016	2017	2015	2016	2017	2015	2016	2017	2015	2016	2017
May		188.5	194.8		145.2	138.6		-0.10			1.72	
Jun	217.2	214.3	224.8	157.3	191.6	181.8	-0.15	-0.24	-0.20	2.40	0.98	1.81
Jul	198.0	185.2	218.1	123	101.0	93.4	-0.02	0	-0.04	2.6	2.89	3.28
Aug	170.4	178.6	177.2	62.3	32.4	39.3	0.11	0.13	0.11	3.33	4.47	4.31
Sep	148.4	140.2	154.1	-24.6	-10.7	-15.4	0.13	0.14	0.08	5.29	4.57	5.40
Oct	89.1	91.4	92.4	-115	-87.1	-86.4	0.23	0.20	0.20	5.67	5.12	5.15
Nov	34.7	34.9	34.3	-140.6	-193.7	-199.5	0.17	0.18	0.24	5.12	6.69	6.51
Dec	17.7	16.6	19.7	-192	-125.3	-148.5	0.26	0.14	0.20	5.78	4.22	4.88

605

610

615

620

625

630

Table 3 Runoff (m³/s) of the three main rivers in Paiku Co basin during the pre-monsoon and post-monsoon seasons between 2015 and 2017 and their total contribution to lake-level increase (mm/day).

Rivers	Runoff-2015		Runoff-2016		Runoff-2017	
	Spring (6.1~6.2)	Autumn (10.6~10.7)	Spring (6.2)	Autumn (10.11~10.13)	Spring (5.25~5.28)	Autumn (10.14~10.16)
Bulaqu	2.3	2.1	0.8	0.7	0.5	0.7
Daqu	0.4	2.8	1.1	1	0.5	1.2
Barixiongqu	0.2	0.4	0.1	0.5	0.1	0.5
Total contribution	0.89	1.64	0.62	0.71	0.62	0.74

Total contribution is calculated according to the total runoff of the three main rivers and lake area. The measuring dates are shown in brackets.
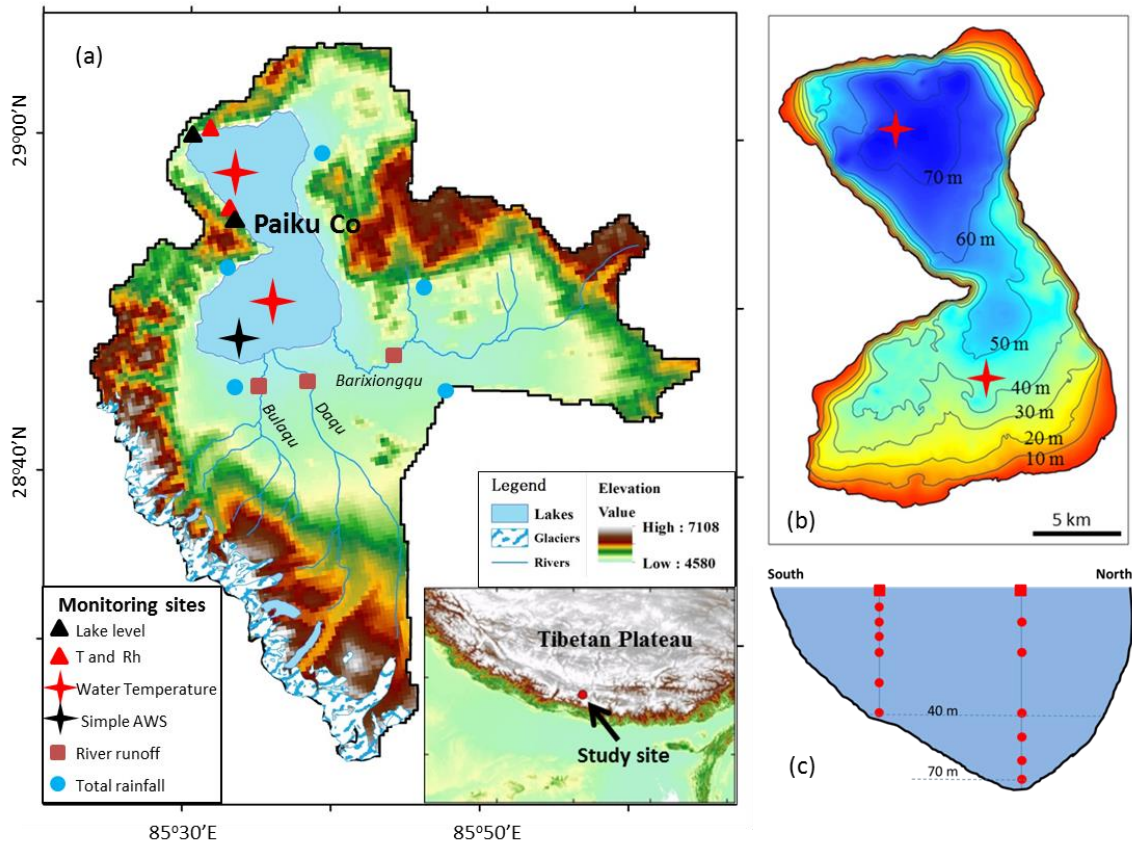
Figure 1: Monitoring sites of lake water budget in Paiku Co basin. (a): Monitoring sites of lake level, hydro-meteorology, water temperature profile, runoff, and total rainfall. (b): The isobath of Paiku Co and the two monitoring sites of water temperature profile. (c): The water temperature monitoring at different water depths.
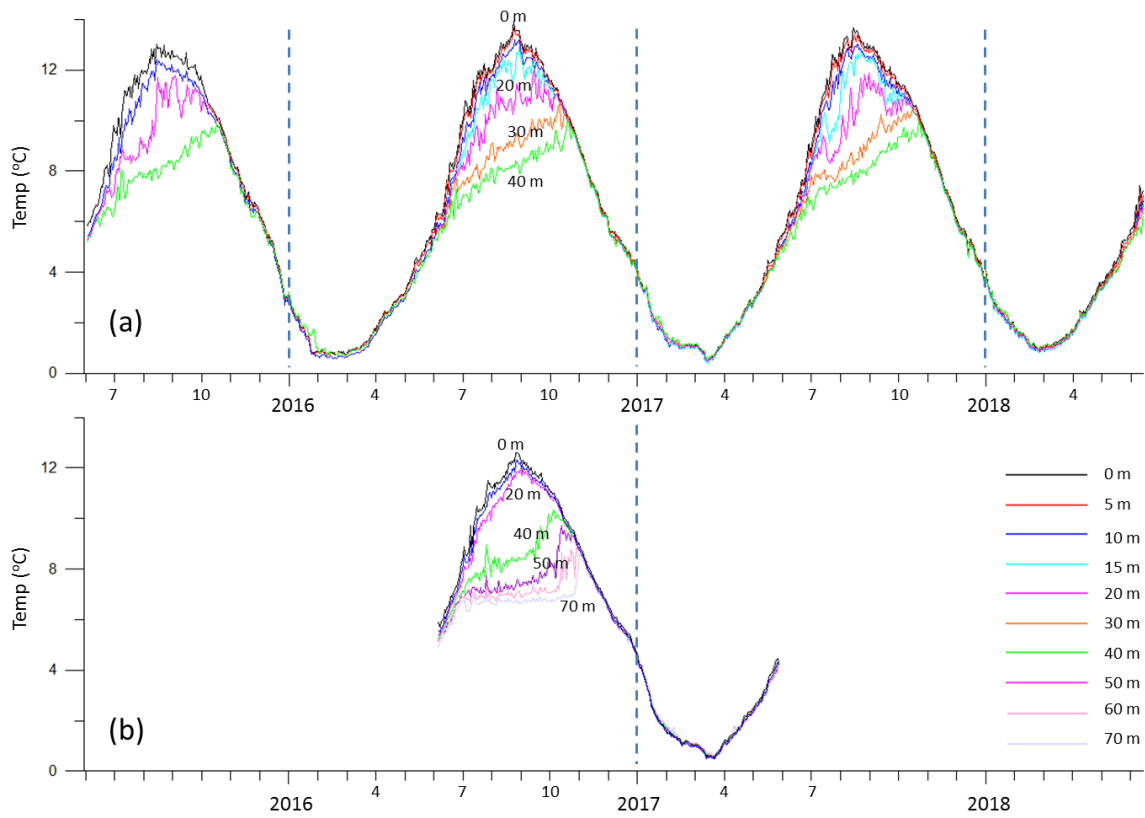
Figure 2: Time series of daily lake water temperature at different water depths in Paiku Co's southern (a) and northern basins.
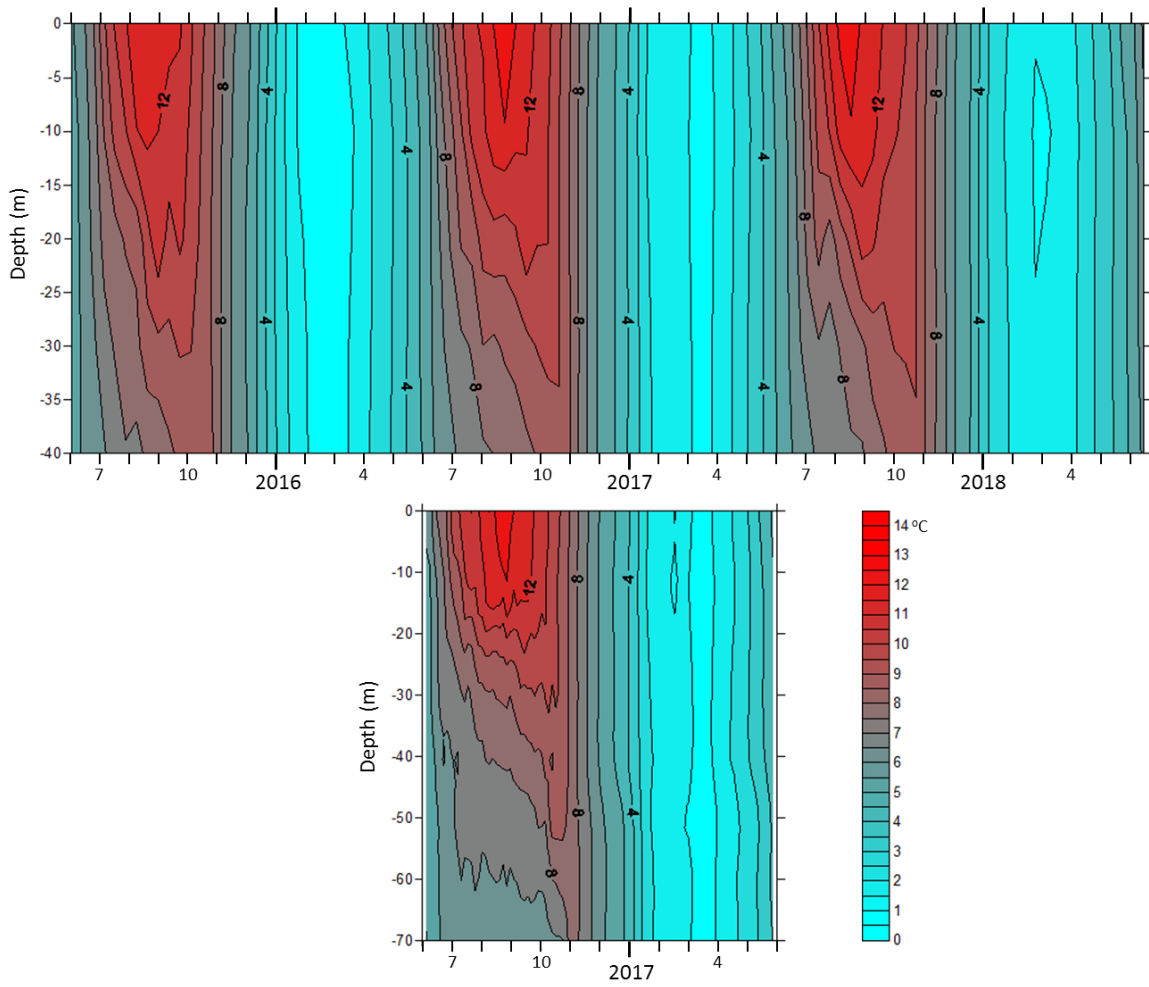
Figure 3: Depth-time diagram of isotherm (°C) in Paiku Co's southern (upper, 42 m in depth) and northern (below, 72 m in depth) basins between June 2015 and May 2018.
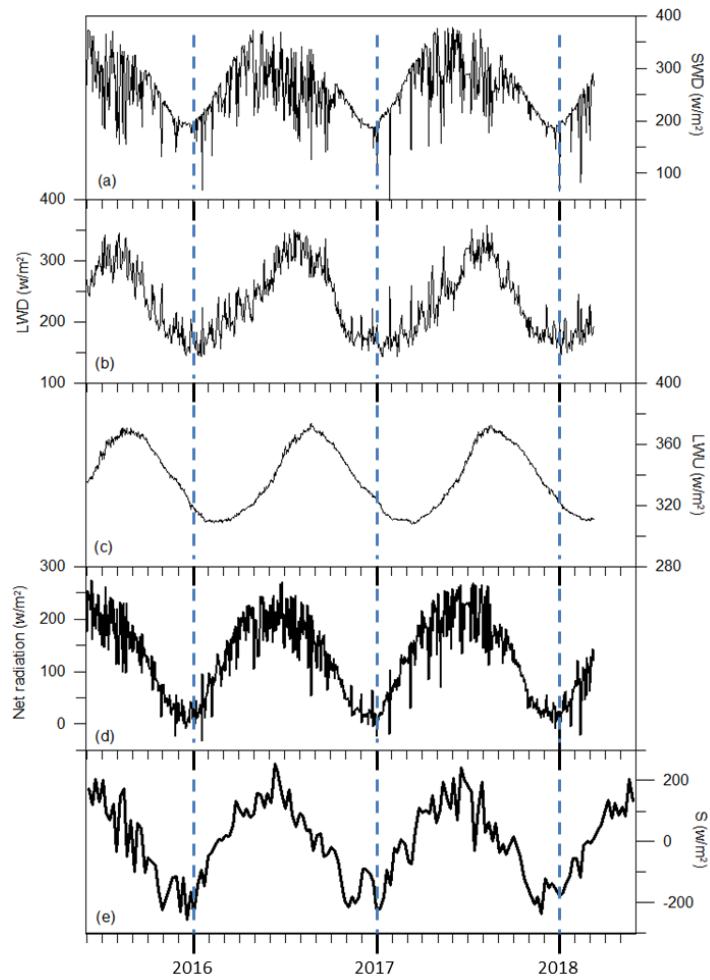
670

Figure 4: The main components of energy budget at the lake surface. (a): Daily solar radiation (SWD), (b): Daily atmospheric longwave radiation to the lake (LWD), (c): Daily long wave radiation emitted from the lake (LWU), (d): Daily net radiation, (e): Weekly changes in lake heat storage (S).

675
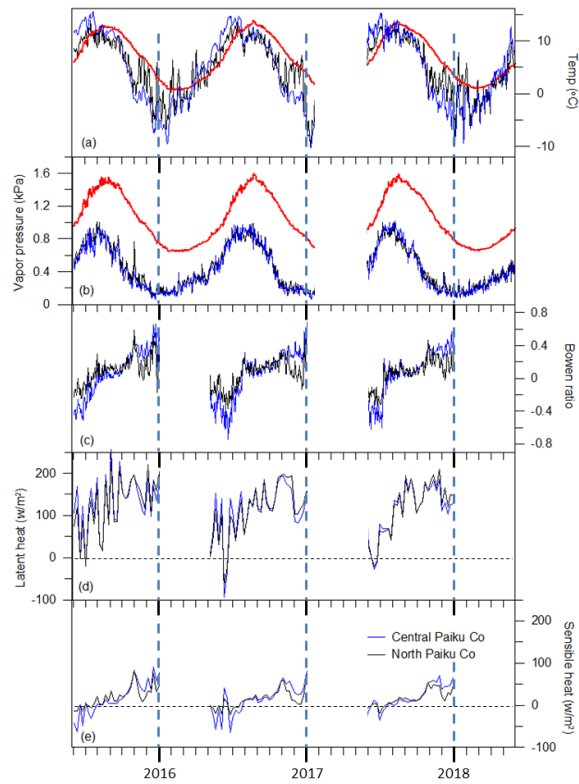
Figure 5: Hydrometeorology and heat fluxes at the lake surface. (a): Daily air temperature and lake surface temperature (red line), (b): Daily actual vapour pressure at lake surface (red line) and the overlying atmosphere, (c): Daily Bowen ratio between May and December, (d-e): Weekly averaged latent and sensible heat fluxes between May and December. For a-e, black lines denote north Paiku Co and blue lines denote central Paiku Co. There was no data available between February and May 2017.

685
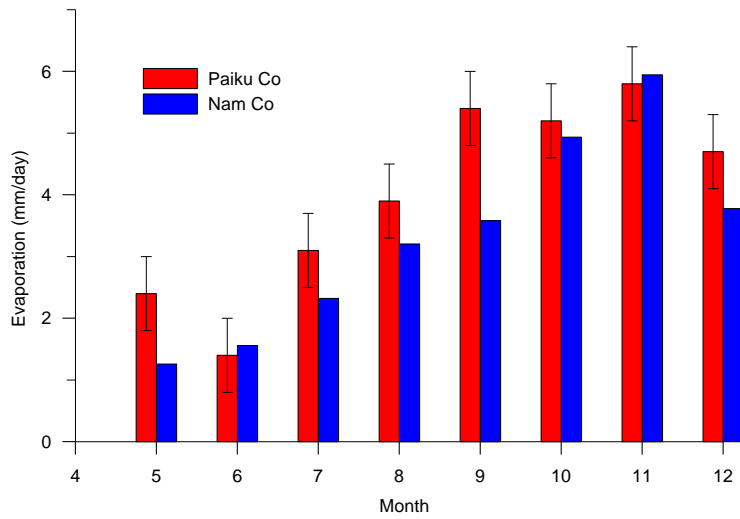
690

Fig. 6 Comparison of monthly lake evaporation at Paiku Co with Nam Co on the central TP. Lake evaporation at Nam Co was determined by using eddy covariance system in the lake center (Wang et al., 2019). The bars denote the uncertainty of lake evaporation at Paiku Co.

695

700

705

710
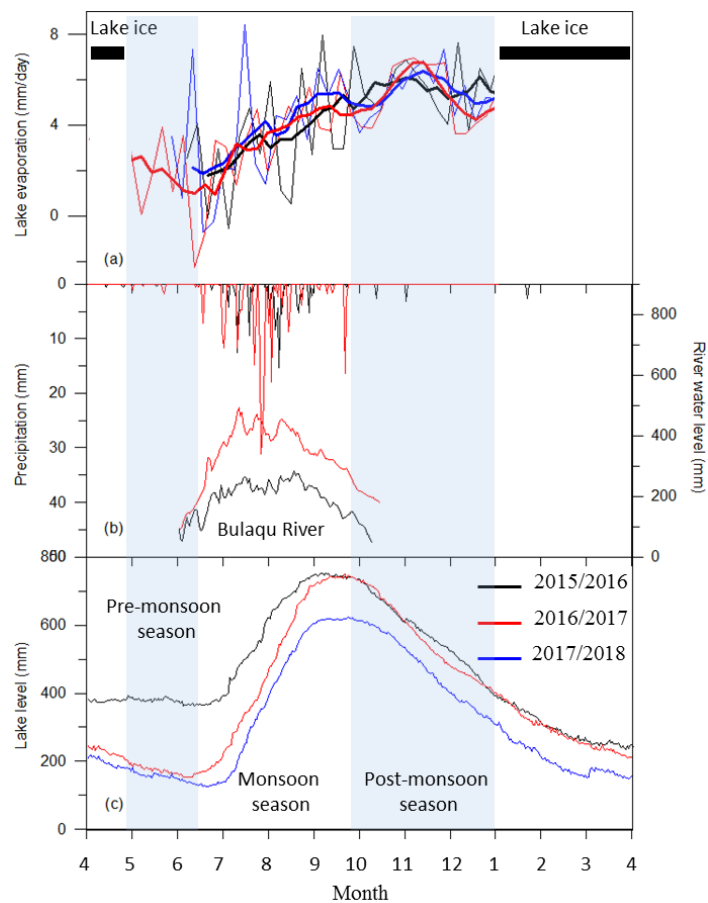
Figure 7: The main components of lake water budget at Paiku Co between 2015 and 2018. (a): Lake evaporation (mm/day) derived from the north shoreline of Paiku Co. (b): Daily precipitation (mm) at Qomolangma station and water level (mm) of Bulaqu River in 2015 and 2016. Note the Y axis (left) of precipitation is reversed. (c): Daily lake level (mm) at Paiku Co. The thick lines (a) denote the 5-point running average. The blue rectangles represent pre-monsoon and post-monsoon seasons periods, respectively.
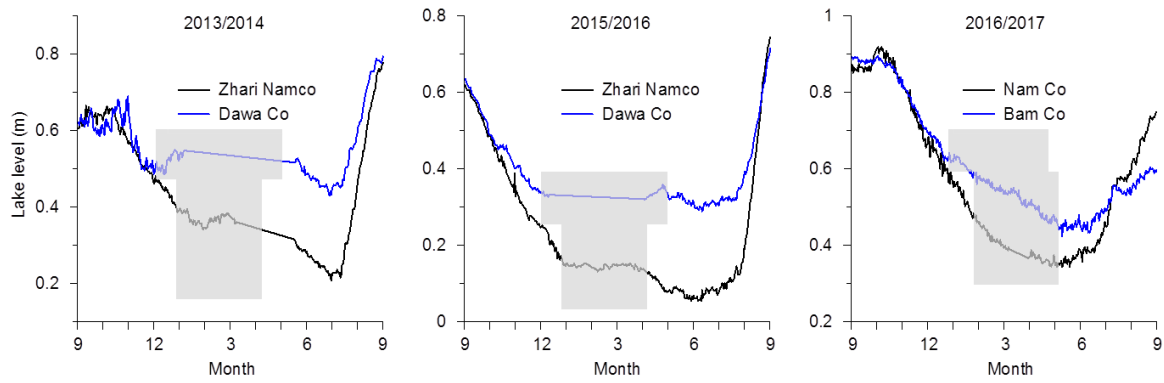
Figure 8: Different amplitude of seasonal lake-level changes between deep and shallow lakes on the central TP.
Relatively deep lakes: Zhari Namco (85.61 ^{o}E, 30.93 ^{o}N) and Nam Co (90.60 ^{o}E, 30.74 ^{o}N); Relatively shallow lakes:
Dawa Co (84.96 ^{o}E, 31.24 ^{o}N) and Bam Co (90.58 ^{o}E, 31.26 ^{o}N). Grey rectangles in each figure represent lake ice
covered periods.
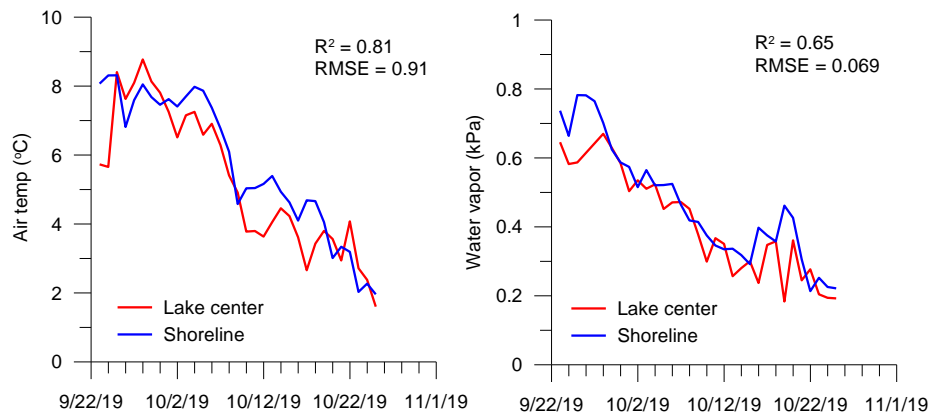
Figure 9: Comparison of daily air temperature and water vapour pressure between shoreline and lake centre during the period of 23/9/2019-25/10/2019.